REPEAT STORM SURGE DISASTERS OF TYPHOON HAIYAN AND ITS 1897 PREDECESSOR IN THE PHILIPPINES

BY JANNELI LEA A. SORIA, ADAM D. SWITZER, CESAR L. VILLANOY, HERMANN M. FRITZ, PRINCESS HOPE T. BILGERA, OLIVIA C. CABRERA, FERNANDO P. SIRINGAN, YVAINNE YACAT-STA. MARIA, RIOVIE D. RAMOS, AND IAN QUINO FERNANDEZ

Typhoon Haiyan's storm surge was about twice the height of the 1897 event in San Pedro Bay, but the two storm surges had similar heights on the open Pacific coast.

Typhoon Haiyan affected more than 16 million people, killed 6,293 people, and destroyed more than 1.1 million dwellings in the central Philippines (NDRRMC 2014). Haiyan is the deadliest typhoon recorded in the Philippines, superseding Tropical Storm Thelma, which struck Ormoc City on the western coast of Leyte Island, in November 1991 (Alojado and Padua 2010; Bacani 2013; Ribera et al. 2008). Globally, Typhoon Haiyan was the deadliest cyclonic event since Cyclone Nargis devastated Myanmar in 2008 (Fritz et al. 2009). The damage to infrastructure and agriculture cost about PHP $40 billion or about USD $900 million (NDRRMC 2014), while the total economic loss reached up to USD 13 billion (Caulderwood 2014). The damage and the death toll from Typhoon Haiyan were particularly high along the coasts surrounding San Pedro Bay on the northwestern margin of the Leyte Gulf primarily due to the storm surge generated by the typhoon. The shallow bathymetry of less than 10-m depth and funnel shape make the coasts of San Pedro Bay inherently susceptible to storm surge (Fig. 1, inset). Additional factors that contributed to local amplification of the storm surge in Leyte Gulf were the orientation of the typhoon track and associated seiches (Mori et al. 2014). Eyewitnesses described the Haiyan storm surge as dramatically worse than any coastal flooding events in recent years (Amadore 2013). Longer historical records,

AFFILIATIONS: SORIA, SWITZER, AND RAMOS—Earth Observatory of Singapore, and Asian School of the Environment, Nanyang Technological University, Singapore; VILLANOY, BILGERA, CABRERA, SIRINGAN, MARIA, AND FERNANDEZ—Marine Science Institute, University of the Philippines, Diliman, Quezon City, Philippines; FRITZ—School of Civil and Environmental Engineering, Georgia Institute of Technology, Atlanta, Georgia
CORRESPONDING AUTHOR: Adam D. Switzer, Earth Observatory of Singapore, Nanyang Technological University, 50 Nanyang Avenue, Singapore 639798, Singapore
E-mail: aswitzer@ntu.edu.sg

Earth Observatory of Singapore Contribution Number 95

The abstract for this article can be found in this issue, following the table of contents.
DOI:10.1175/BAMS-D-14-00245.1

A supplement to this article is available online (10.1175/BAMS-D-14-00245.2)

In final form 29 May 2015

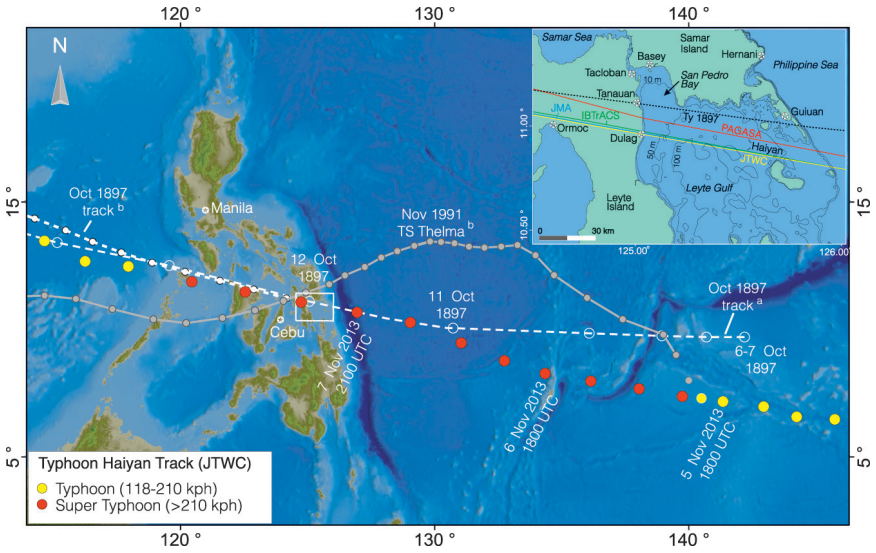

Fig. 1. Storm tracks of three deadly typhoons crossing the central Philippines: Ty 1897, Nov 1991 Tropical Storm Thelma, and Nov 2013 Super Typhoon Haiyan. Typhoon track sources: (a) Algué (1898) and (b) International Best Track Archive for Climate Stewardship (IBTrACS) database of Knapp et al. (2010). The inset shows the comparative tracks of Ty 1897 (black dashed line) and Haiyan (colored solid lines) across Leyte Gulf.

however, reveal a comparable predecessor to Typhoon Haiyan (Algué 1898). In October 1897, an unnamed typhoon, which for brevity will be henceforth referred to as Ty 1897, took a path across Leyte Gulf that was almost parallel to Typhoon Haiyan's but offset to the north by ~6 km (Fig. 1). The similar track enables direct comparisons of the two typhoons and the storm surges. Here, we first characterize the destructiveness of Typhoon Haiyan before considering the importance of the 1897 predecessor in understanding storm surge hazard in the region.

TYPHOON HAIYAN. On 2 November 2013, a broad low pressure area formed in the western Pacific, to the east of Micronesia (Joint Typhoon Warning Center 2014). By 0600 UTC 3 November, it had developed into a tropical depression. At 0000 UTC 4 November, the system had attained tropical storm strength and was named Haiyan. It rapidly strengthened into a typhoon and moved west toward the Philippines (Fig. 1), and it was given the local name of Yolanda (NDRRMC 2013a). By 6 November, Haiyan's 1-min maximum sustained winds had intensified to an estimated 241 km h^{-1}, classified by the Joint Typhoon Warning Center (JTWC) as a super typhoon. To avoid ambiguity in the definition of "super typhoon," we will conform to the traditional classification of tropical cyclones (World Meteorological Organization 2015) in the Pacific region with "typhoon."

On its final northwestward approach to the Philippines, Haiyan steadily intensified until it reached the peak intensity of ~895 hPa minimum central pressure. This peak intensity was estimated by the JTWC and the Japan Meteorological Agency (JMA) from cloud patterns recognized on visible and infrared satellite images, in the absence of ground and in situ instruments. In Guiuan municipality on Samar Island, Doppler radar data of the Philippine Atmospheric, Geophysical and Astronomical Services Administration (PAGASA) indicated that just before landfall, at 2000 UTC 7 November [0400 Philippine Time (PHT) 8 November], Haiyan attained a minimum central pressure of 910 hPa and winds at 160 km h^{-1} with gusts of ~195 km h^{-1} (Paciente 2014). Extreme winds destroyed the Guiuan Doppler radar station about 16 min later. At 2040 UTC 7 November (0440 PHT 8 November), Haiyan crossed the small islands off the southeast tip of Samar Island, near Guiuan. Haiyan then continued westward across the Leyte Gulf to its main landfall south of Tolosa, Leyte Island, at 2300 UTC 7 November (0700 PHT 8 November), as captured by another PAGASA Doppler radar station in Cebu. Typhoon Haiyan then made four subsequent landfalls as it crossed the central Philippines (NDRRMC 2013b).

MATERIAL AND METHODS. We evaluated eyewitness accounts, video recordings, field measurements, and storm surge model hydrographs to document the flow depths, surge heights, timing, and peak flood duration during Typhoon Haiyan as well as the resulting damage. Other post-Haiyan field survey reports focused on the inundation characteristics and the impact on coastal structures (Mas et al. 2015; Tajima et al. 2014). Here, we place Typhoon Haiyan's storm surge into historical context by comparing it with the similar Ty 1897 event (Algué 1898).

Field survey. The initial field survey of the coastal areas surrounding San Pedro Bay was conducted from 23

to 28 November 2013, as soon as relief operations and the security situation permitted access to the hardest hit areas. We recorded 73 eyewitness accounts (Table ES1; more information can be found online at http://dx.doi.org/10.1175/BAMS-D-14-00245.2) on the maximum flow depth, the timing of the initial rise, and peak and subsidence of the flood, along with wind and wave observations. Collected data were used to validate the timing and heights simulated by our storm surge models. Subsequent surveys from 16 to 25 January, 12 to 19 May, and 2 to 10 June 2014 encompassed larger and more remote areas, including coastal settlements in southern Samar facing the Leyte Gulf and the Philippine Sea of the western Pacific (Fig. 2; Table 1). To record distances and build cross-shore elevation profiles from the water surface at the shoreline to the inundation limit, water marks were located and measured with a Trimble global positioning system (GPS) rover connected via Bluetooth to a Lasercraft XLRic laser range finder (Fritz et al. 2012). At each site, high water marks such as mud lines on buildings, scars on the bark of trees, and rafted debris were evaluated using established protocols (Fritz et al. 2007; UNESCO 2014). In inhabited areas, the water marks were discussed with eyewitnesses to constrain still water levels, estimate the contribution of storm waves, and remove bias from localized splashup atop the surge. The high water measurements, based on different indicators at corresponding locations, tended to be consistent and have an individual confidence of ±0.1 m. During post-survey processing, the measurements were differentially corrected with our daily setup of the local Ashtech base station and corrected for tide level at the time of peak storm surge on the basis of tide predictions provided by XTide 2, an open-source software of Flater (1998). How the Ty 1897 storm surge heights were measured remains unknown, but it is highly likely that surge heights

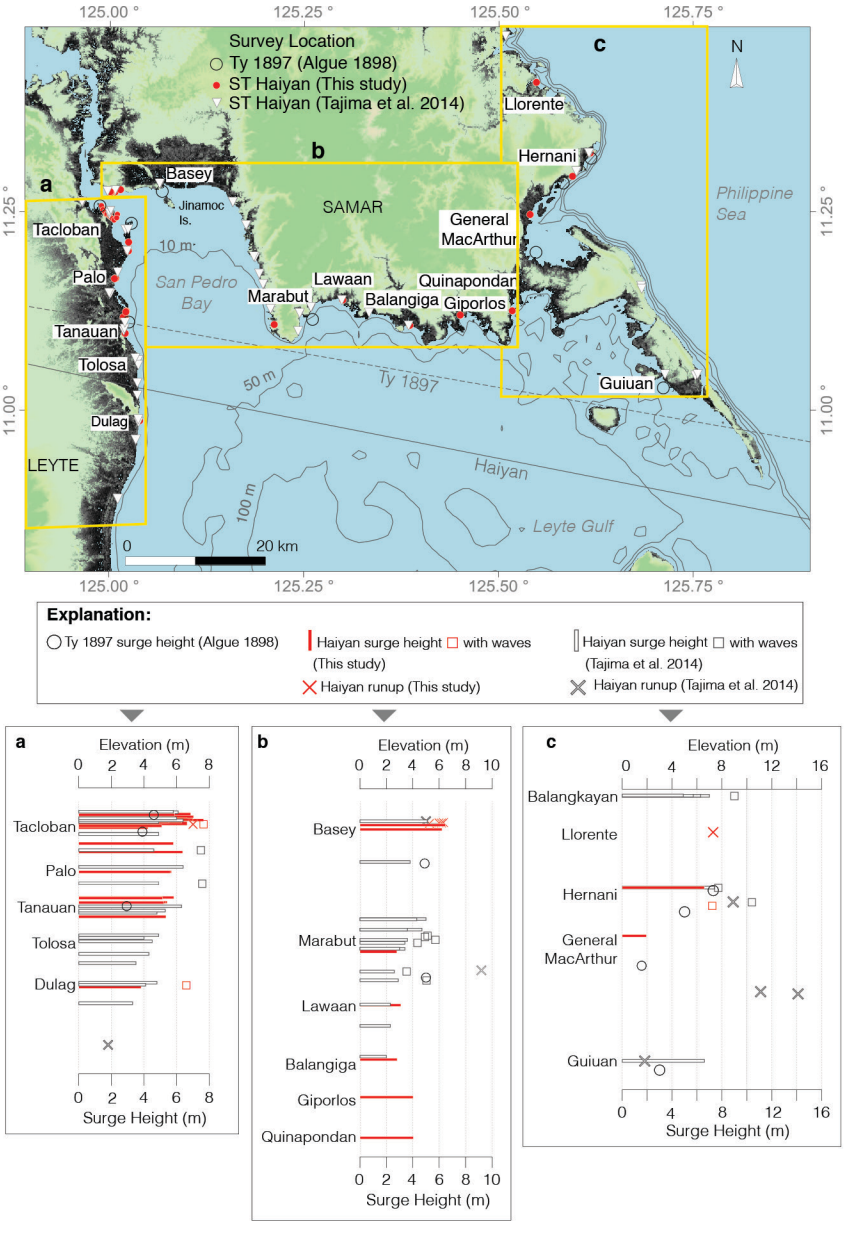

Figure 2.

Fig. 2. Maximum storm surge heights, surge with waves, and runup points of Typhoon Haiyan measured in the field across the coastal communities in eastern Leyte (a), and Samar (b) and (c). Surge heights of Ty 1897 from Algue (1898) are also included for comparison. The terrain map is a modified NASA land elevation radar image; dark shaded areas are ≤ 10 m, above sea level.

Table 1. Measured maximum storm surge heights and run-up points of Super Typhoon Haiyan in eastern Leyte and the southern Samar Islands. The code for measurements is as follows: z is terrain elevation, *h* is the flow depth above terrain, z + *h* is the elevation of the watermark relative to normal predicted tide level at time of peak flooding, and *R* is run-up or elevation at the limit of inundation. The code for watermarks is as follows: TL is the trimline, WS is wave splash, FL is the flood line, EW is eyewitness, RD is rafted debris, SH is ship, MI is mud line inside, MO is mud line outside, and WL is wrack line.

Point	Location	Latitude (°N)	Longitude (°E)	z (m)	h (m)	z + *h* (m)	*R* (m)	Date and time surveyed (PHT)		Watermark
1	Dulag (San Jose)	10.9869	125.0393	2.22	4.60	6.82		20 Jan 2014	1223	TL, WS
2	Dulag (San Jose)	10.9868	125.0393	2.82	1.00	3.82		20 Jan 2014	1232	FL, EW
3	Tanauan (Cabuynan)	11.0969	125.0207	1.64	3.70	5.34		20 Jan 2014	1514	TL, EW
4	Tanauan (Magay)	11.1172	125.0205	2.52	2.90	5.42		20 Jan 2014	1621	EW
5	Tanauan (Magay)	11.1165	125.0199	2.22	3.00	5.22		20 Jan 2014	1630	EW
6	Tanauan (Magay)	11.1173	125.0182	2.62	2.70	5.32		20 Jan 2014	1641	RD
7	Hernani (town proper)	11.3236	125.6177	3.88	2.70	6.58		21 Jan 2014	1332	FL, EW
8	Tacloban (Anibong)	11.2542	124.9906	3.05	3.80	6.85		22 Jan 2014	1101	SH
9	Tacloban (Anibong)	11.2543	124.9905	5.84	1.20	7.04		22 Jan 2014	1052	TL, EW
10	Tacloban (Anibong)	11.2575	124.9891	3.09	2.80	5.89		22 Jan 2014	1123	TL, EW
11	Tacloban	11.2523	124.9909	4.09	1.00	5.09		22 Jan 2014	1138	MO, EW
12	Tacloban	11.2494	124.9934	4.10	2.90	7.00		22 Jan 2014	1235	MI, EW
13	Tacloban	11.2465	124.9952	2.07	2.50	4.57		22 Jan 2014	1251	MI, EW
14	Tacloban	11.2470	124.9961	2.94	3.70	6.64		22 Jan 2014	1307	EW
15	Tacloban	11.2443	124.9991	2.39	1.60	3.99		22 Jan 2014	1427	MI
16	Tacloban	11.2437	125.0001	1.92	1.90	3.82		22 Jan 2014	1438	MI, EW
17	Tacloban	11.2423	125.0018	2.49	1.60	4.09		22 Jan 2014	1448	MI, EW
18	Tacloban	11.2411	125.0032	2.69	1.55	4.24		22 Jan 2014	1455	MI, EW
19	Tacloban	11.2394	125.0053	2.19	2.90	5.09		22 Jan 2014	1511	MI, EW
20	Tacloban	11.2421	125.0085	7.48	0.40	7.88		22 Jan 2014	1542	MO, WS
21	Tacloban	11.2421	125.0086	7.01			7.01	22 Jan 2014	1552	WL, EW
22	Tacloban	11.2464	125.0095	4.22	2.10	6.32		22 Jan 2014	1610	TL
23	Tacloban	11.2464	125.0095	4.22	1.30	5.52		22 Jan 2014	1611	MI, EW
24	Tacloban	11.2488	125.0004	3.06	4.60	7.66		22 Jan 2014	1652	TL, EW
25	Basey (San Antonio)	11.2731	125.0030	5.26			5.26	23 Jan 2014	0944	WL
26	Basey (San Antonio)	11.2734	125.0023	6.17			6.17	23 Jan 2014	0956	WL
27	Basey (San Antonio)	11.2739	125.0021	5.99			5.99	23 Jan 2014	0947	WL

28	Basey (San Antonio)	11.2750	125.0015	6.32			6.32	23 Jan 2014	0959	WL
29	Basey (San Antonio)	11.2745	125.0077	2.76	3.70	6.46		23 Jan 2014	1033	TL, EW
30	Basey (San Antonio)	11.2775	125.0147	3.31	2.90	6.21		23 Jan 2014	1124	MO, WS
31	Marabut	11.1078	125.2120	1.58	1.20	2.78		23 Jan 2014	1324	EW
32	Hernani (town proper)	11.3236	125.6177	3.88	2.70	6.58		21 Jan 2014	1332	EW
33	Hernani (Batang)	11.2943	125.5948	6.22	1.30	7.52		23 Jan 2014	1508	MO, EW
34	General MacArthur	11.2463	125.5404	1.49	0.45	1.94		23 Jan 2014	1548	MO, EW
35	Quinapondan/Santo Niño	11.1252	125.5175	1.64	2.40	4.04		23 Jan 2014	1653	MO, EW
36	Giporlos	11.1199	125.4507	1.62	2.40	4.02		23 Jan 2014	1722	MO, EW
37	Balangiga	11.1068	125.3860	1.31	1.50	2.81		23 Jan 2014	1739	MO, EW
38	Lawaan	11.1387	125.3000	1.20	1.90	3.10		23 Jan 2014	1807	MO, EW
39	Palo (San Fernando)	11.1661	125.0085	1.98	3.70	5.68		24 Jan 2014	1641	TL, EW
40	Palo (San Fernando)	11.1656	125.0070	2.61	3.00	5.61		24 Jan 2014	1653	TL, EW
41	Tacloban (south of airport)	11.2005	125.0249	3.47	2.90	6.37		24 Jan 2014	1716	TL, EW
42	Tacloban (bay south of airport)	11.2115	125.0251	2.10	3.70	5.80		24 Jan 2014	1735	TL, EW
43	Tanauan (Santa Cruz)	11.1247	125.0220	1.73	4.10	5.83		24 Jan 2014	1321	MO, EW
44	Tanauan (Santa Cruz)	11.1237	125.0215	1.73	3.40	5.13		24 Jan 2014	1326	MO, EW
45	Llorente	11.4124	125.5485	7.29			7.29	10 Jun 2014	1409	EW

were simply referenced to the mean sea level at the time of survey. The difference between the mean sea level and the sea level at the time of peak flood during Ty 1897 implies that the accuracy of surge height measurements is in the range of ±0.3 m. Algué (1898) lacks description on the surge height indicators, but additional uncertainties can be potentially contributed by storm waves.

Storm surge modeling of Typhoon Haiyan. The Typhoon Haiyan storm surge in Leyte Gulf and San Pedro Bay was simulated using the open-source Delft3D Flow (Lesser et al. 2004) with a MATLAB-based graphical user interface called Dashboard.[1] A curvilinear grid is used with a minimum resolution of 200 m and a maximum resolution of 1.2 km. The domain encompasses the whole Leyte Gulf and extends into the San Juanico Strait to the north (Fig. 3a). The bathymetry of the model domain was acquired from digitized navigational charts (National Mapping and Resource Information Authority 1980). The maximum depths are found near the Leyte Gulf mouth, and the embayment shallows northward toward the San Juanico Strait (Fig. 3b). Open boundary conditions are astronomic tides using eight dominant constituents (M_2, S_2, N_2, K_2, K_1, O_1, P_1, and Q_1) extracted and interpolated from the Ocean Topography Experiment (TOPEX7.2) global tidal model (Egbert and Erofeeva 2002) using the Dashboard tide database toolbox. The tidal pattern in San Juanico Strait interacting with the Samar Sea differs from the tidal pattern at Guiuan station driven by the Philippine Sea (Fig. 3c). The complex tidal interaction highlights the need for accurate bathymetry of Leyte Gulf and San Juanico Strait to properly simulate the tides in Tacloban.

Typhoon wind fields for the modeling were generated from the typhoon track data of the JTWC. We recognize an approximately 6-km offset between the JTWC typhoon track from the Doppler radar–derived track from PAGASA (Fig. 1, inset), but JTWC provides more continuous along-track wind data, required in the model. The model wind

[1] http://publicwiki.deltares.nl/display/OET/DelftDashboard

files were generated by the Delft Dashboard tropical cyclone toolbox using the model by Holland (1980) and interpolated onto the computational grid. The model was initialized by wind and tide conditions at 0000 UTC 5 November 2013 and allowed to run until 2400 UTC 11 November 2013. Sea level and current outputs were saved at 1-min intervals between 1900 UTC 7 November and 0600 UTC 8 November. An earlier model of Bricker et al. (2014) used the same Delft3D software with JMA wind data forcing and a Quiring's relationship of maximum wind radius. Their model yielded a maximum water level of less than 6 m in Tacloban.

Storm surge modeling of Ty 1897. To model the likely storm surge generated by Ty 1897, we used the same grid and boundary forcing conditions of Typhoon Haiyan, but with tides simulated from 10 to 12 October 1897. Algué (1898) reported pressures and winds recorded in various parts of the Philippines during Ty 1897, but the Dashboard typhoon module requires along-track minimum central pressures and maximum winds. This requirement limited us to use only the data recorded in areas directly hit by the eye of Ty 1897: the in situ barometric pressures measured at Guiuan and Tanauan. Apart from these two locations, no instrumental record on the typhoon eye exists. The minimum pressures before landfall in Guiuan and after landfall in Tanauan were estimated considering the values for Ty 1897 and Typhoon Haiyan. Barometric records in Guiuan and Tanauan indicate a less intense Ty 1897 at landfall than Typhoon Haiyan. To account for the weaker intensity of Ty 1897, we took the pressure difference between Typhoon Haiyan and Ty 1897 in Guiuan and in Tanauan, and the delta values were then subtracted from the Typhoon Haiyan pressure values.

Given the barometric records of Ty 1897 in Guiuan and Tanauan, a range of wind speed values were derived from empirical wind–pressure relationships using the storm-mapping table summarized by Nakazawa and Hoshino (2009) for the western North Pacific region (Table 2). Due to the limited instrumental data on Ty 1897 we opted to use in our model the wind speed values derived from Atkinson and Holliday (1977), which is the most direct method among the wind-pressure relationship equations. Knaff and Zehr (2007) emphasized the uncertainties inherent in the regression method of Atkinson and Holliday (1977) in estimating wind speeds of tropical cyclones over the northwest Pacific. Despite the reliability concerns, the maximum wind speed estimates for Ty 1897 using Atkinson and Holliday (1977) still yielded values similar or within the range of the mean standard error [6–9 kt (1 kt = 0.5144 m s^{-1})] of other established robust wind–pressure relationships.

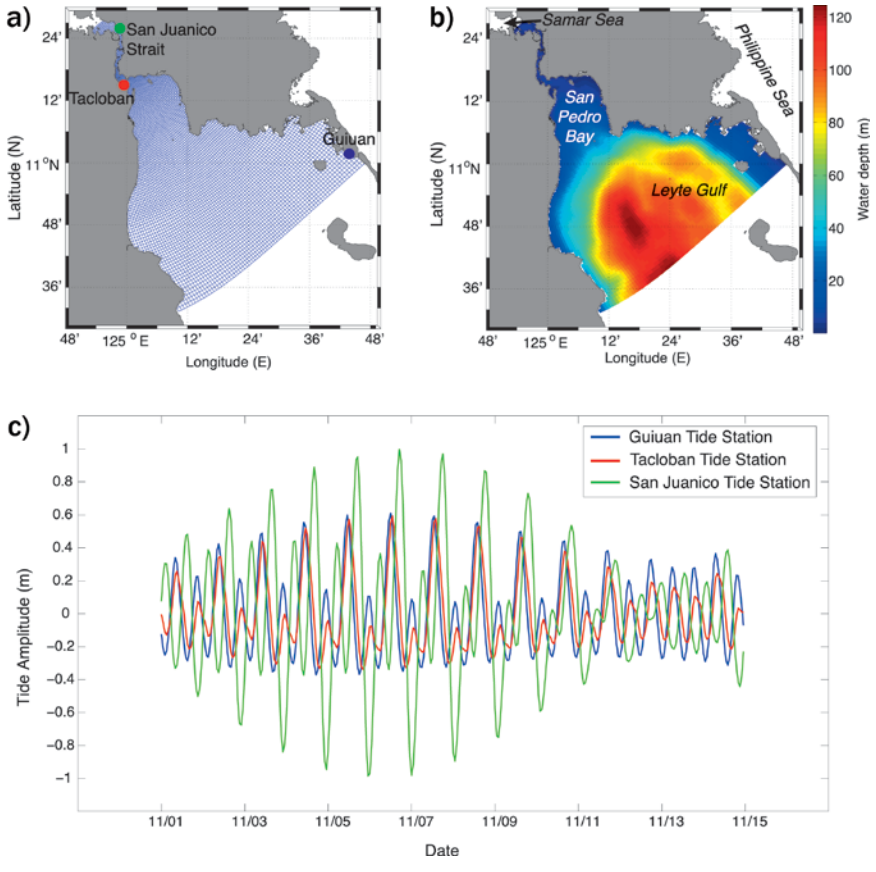

Fig. 3. Geographical coverage, bathymetry, and tidal conditions of Leyte Gulf used in the model. (a) The model domain is a curvilinear grid with 200-m to 1.2-km resolution. (b) Leyte Gulf bathymetry generated from digitized navigational charts with 100-m to 1-km resolution. (c) Predicted water levels from San Juanico Strait, Tacloban City, and Guiuan, Samar.

TYPHOON 1897 VERSUS TYPHOON HAIYAN. *Typhoon track and forward speed.* The reconstructed track of Ty 1897 (Figs. 1, 2) was

Table 2. Minimum barometric pressure of Ty 1897 recorded in Guiuan and Tanuan and the corresponding CI number and maximum wind speeds.

Parameters/location	Guiuan	Tanauan (initial)	Tanauan (corrected)
Time and date	0815 PHT 12 Oct 1897	1110 PHT 12 Oct 1897	1110 PHT 12 Oct 1897
Minimum central pressure (mm)	710	704	694
Minimum central pressure (hPa)	947	938	925
Observed wind condition	Relative calm[a]	Absolute calm	Absolute calm
1-min maximum sustained winds [kt (km h^{-1})] (Atkinson and Holliday 1977)	96 (179)	105 (194)	115 (212)
CI (Dvorak 1975)	6	6.5	7
CI (Dvorak 1984)	5.5	6	6
1-min maximum sustained winds [kt (km h^{-1})] (Dvorak 1984)	102 (189)	115 (213)	115 (213)
CI (Koba et al. 1990)	5.5	6	6.5
10-min maximum sustained winds [kt (km h^{-1})] (Koba 1990)	85 (157)	93 (172)	100 (185)

[a] The relatively calm wind condition recorded in Guiuan indicates that the eye passed close but not directly over the recording site. As such the Guiuan dataset should be considered a near-minimum value.

adopted from Algué (1898) based on the synthesis report containing maps and compilation of barometric curves. Instrumental records for the historical Ty 1897 came from modified aneroid barometers established by Jesuit priests on land (at churches) and at sea (on ships) in different locations of the Philippine Archipelago. The observed pressure, wind direction, and temperature were used to establish the distance and direction of the vortex (eye) of the typhoon from the observer (Algué 1904; Udías 1996). Algué's map was georeferenced to a regional map derived from a 90 m × 90 m resolution satellite radar image, and then the typhoon track was digitized. Given the different resolutions between Algué's map and the regional map, we expect that the digitized track has uncertainties of ~1 km in the north–south direction and ~2 km in the east–west direction.

Upon evaluating the pressure and wind observations, Algué (1898) estimated the landfall timing and the forward speed of Ty 1897 between Guiuan and Tanauan. Ty 1897 made its initial landfall ~10 km south of Guiuan shortly after 0800 PHT 12 October 1897 (0000 UTC 12 October). At landfall, the barometer in Guiuan registered the lowest pressure at 710 mm (947 hPa), simultaneous with the observed relatively calm winds. The relatively calm wind condition indicates an eye passage in close proximity but not directly over the recording site. As such, the Guiuan dataset should be considered only as a near-minimum value. The typhoon continued westward almost following along the northern coastline of Leyte Gulf. At about 1100 PHT 12 October 1897 (0300 UTC 12 October) the eye of the typhoon was about 21 km north-northeast (NNE) of Dulag, and 13 km south-southeast (SSE) of Tacloban, before it made a second landfall in Tanuan shortly after 1100 PHT. At landfall, the barometer in Tanauan registered the lowest pressure of 704 mm equivalent to 938 hPa, but after further analysis was lowered to 694 mm equivalent to 925 hPa (Algué 1898, 1904). Simultaneous with the lowest pressure was an absolute calm wind lasting for about 40 min. To the north, the adjacent town of Palo also experienced the zone of absolute calm but only for 10 min. The longer duration of absolute calm in Tanauan compared to Palo suggests that Tanauan was located closer to the center of the typhoon's eye. In a span of 2.5 h, Ty 1897 traversed about 43 geographical miles (~80 km) between Guiuan and Tanuan, equivalent to a forward speed of about 17 mi h^{-1} or 28 km h^{-1} (Algué 1898, p. 66). According to Algué's map, Ty 1897 made subsequent landfalls on three islands across the central Philippines before it exited into the South China Sea.

The Jesuits ground-based method of instrumental recording and monitoring of typhoons to establish the track and intensity prevailed for many decades (Udías 1996) until it was replaced by reconnaissance aircraft, radar, and satellite observations toward the midtwentieth century (Emanuel 2005b; Velden et al. 2006). Today, weather services combine instrumental recordings with satellite-based observations of the cloud patterns in visible and infrared satellite images to establish a central location of a typhoon and to estimate typhoon intensities. At the forefront of this satellite-based method of tropical cyclone intensity was Dvorak (1975). The Dvorak method originally

developed for Atlantic conditions has been adopted and applied to other ocean basins that have different atmospheric conditions like the Pacific (e.g., Velden et al. 2006; Knaff and Zehr 2007; Lander et al. 2014). Unfortunately, there is no unified operational method among weather agencies for tracking and assigning typhoon intensities, and as such, the reported track and intensity of one storm are commonly variable. This was the case with Typhoon Haiyan, where the tracks across Leyte Gulf released by JMA and JTWC are consistently offset ~6 km to the south of the PAGASA Doppler radar-based track. The PAGASA track, however, appears more consistent with the local field observation and ground truthing (Morgerman 2014). We note that based on the PAGASA typhoon track, Typhoon Haiyan moved from Guiuan westward to Tolosa at about 43 km h^{-1} or about 1.5 times faster than Ty 1897.

Typhoon intensity and size. The wide range of instrumental recording through history and the variety of operational wind–pressure relationships among meteorological agencies make typhoon intensity classification based on the maximum wind speed inherently uncertain (Knaff and Zehr 2007; Nakazawa and Hoshino 2009). To address the issues arising from the wind speed–derived typhoon intensity, Knapp and Kruk (2010) and Kruk et al. (2011) proposed the use of current intensity (CI) in comparing typhoons, particularly in establishing trends of tropical typhoon intensities. Kruk et al. (2011) recognized that because of the imagery interpretation of contemporary typhoons, the satellite-derived intensity *T* number when converted to CI could result in intensity differences of 0.5 on the CI scale. Meanwhile, the primary sources of uncertainty for the pressure-derived intensity of historical typhoons such as Ty 1897 arise from the sparse recordings and possible instrumental errors. The historic correction of ~13 hPa applied to the minimum pressure of Ty 1897 on the Tanauan barometer record may give some indication of the magnitude of instrumental errors. For intense typhoons like Ty 1897, the historic correction corresponds to a difference of 0.5 on the CI scale, which is of similar magnitude as the uncertainty of satellite-derived CI. Hence, the corresponding CI numbers for Ty 1897 and Typhoon Haiyan may provide a reasonable metric to compare the intensity between these two typhoons.

As discussed previously, the observed lowest pressure and absolute calm wind of Ty 1897 consistently indicate that the typhoon eye passed directly over Tanauan. Taking the minimum pressure of 925 hPa as the closest approximation of the central minimum pressure, Ty 1897 was assigned an equivalent CI number of 6–7 upon landfall. For Typhoon Haiyan, ground instruments only recorded near-minimum pressures. The Doppler radar in Guiuan registered a mean sea level pressure of ~940 hPa before it was totally destroyed at the peak intensity of the typhoon (IRIDeS 2014). Independent measurements of PAGASA and Morgerman (2014) indicate lowest pressure at 960 hPa in Tacloban City, which was located on the northern eyewall of the typhoon, 24 km away from Typhoon Haiyan's center. In contrast, using the satellite-based Dvorak technique Typhoon Haiyan has a signature typhoon number of T8.0 (Lander et al. 2014), which corresponds to a CI number of 8, the highest on the scale. As such, the CI 8 Typhoon Haiyan was more intense than the CI 6 to 7 of Ty 1897.

Not only was Typhoon Haiyan more intense, it was also larger than Ty 1897 based on the eyewall size. Morgerman (2014) corroborated the eye of Typhoon Haiyan based on wind observations of eyewitnesses and a radar image, indicating a 13-km radius of the eyewall. In contrast, the Jesuit approach based on the zones of absolute and relative calm winds as indicators of the relative location of the typhoon eye results in an eyewall radius of 6–10 km for Ty 1897.

Given the contrasting operational methods between 1897 and 2013, it remains difficult to directly compare Typhoon Haiyan and Ty 1897 with absolute certainty. The available meteorological parameters, however, suggest that Typhoon Haiyan and Ty 1897 were nearly identical based on the trajectory, while characteristic differences prevailed concerning other aspects. Typhoon Haiyan followed a parallel track direction with a ~6-km offset to the south of Ty 1897. Typhoon Haiyan was more intense, had wider eyewall coverage, and was moving faster than Ty 1897. The possible effects of the slight variations in track, minimum central pressure, estimated maximum winds, and forward movement between the two typhoons on the storm surge characteristics will be explored in the following sections.

TYPHOON 1897 AND TYPHOON HAIYAN STORM SURGES.

Posttyphoon field measurements. The Ty 1897 storm surge measurements of Algué (1898) were based on eyewitness accounts (Fig. 2). These field measurements indicate inundation heights exceeding 4 m in most places with a maximum height of over 7 m on the open sea coast at Hernani (Fig. 2c). Along San Pedro Bay in Basey (Fig. 2b), the water gradually rose and reached a maximum level

of 4.9 m. The peak flooding corresponded with the most violent winds from the southeast. In the nearby coast of Tacloban (Fig. 2a), water rose between 3.9 and 4.6 m. The peak flooding coincided with the winds blowing from the east to east-southeast, directly perpendicular to the Tacloban coast. In close proximity to the eye of Ty 1897 at Tanauan and Tolosa (Fig. 2a), the water rose to 3 m.

Algué's "Ola del Huracán" or hurricane wave was the elevation of the sea, with the surface forming like a warp pyramid whose peak approximately corresponds to the vortex (eye) of the typhoon, analogous to the water surface being sucked by a vacuum pump (Algué 1898, p. 9). Moving with the typhoon, this huge wave, when launched against the shore, makes the water rise to an extraordinary height, causing severe flooding and extensive destruction (Algué 1898, p. 10). We interpret this description as equivalent to what we now call "storm surge." Algué overestimated the contribution of the pressure drop over the wind field as the primary contributor to the significant rise of the sea surface because of the different locations of the eye and the areas where water elevations were highest. The sea rose to about 3 m in Guiuan and Tanauan, but the rise was highest at Hernani, Basey, and Tacloban on the typhoon's strong side to the north of the typhoon eye. The peak flooding during Ty 1897 at each of these sites consistently coincided with winds blowing directly perpendicular toward the coastline. Contrary to Algué's attribution of the surge solely to the low central pressure, the wind field was the primary driver of the storm surge (Emanuel 2005a).

The measured high water marks after Typhoon Haiyan (Fig. 2) were separately classified into maximum surge heights and surge plus storm waves. For a wider and denser spatial coverage, we combined our field measurements with the survey of Tajima et al. (2014). In both surveys, each high water mark indicator was referenced to the reconstructed tide level at the time of peak flooding. Heights differed by as much as 1 m at slightly different locations. Discrepancies of up to 2 m at corresponding locations were attributed to short-period storm waves superimposed on top of the surge. High water marks with significant storm-wave contributions were carefully identified based on eyewitness accounts, the type of physical watermark, and the inland location. Surge height measurements from different high water mark indicators in both surveys were mostly consistent.

At Tacloban, located some 23 km to the north of Haiyan's track (Fig. 2a), the characteristic height of the storm surge peak was 7 m. Wave contributions raised high water marks up to almost 8 m in Tacloban and Palo. On the more open and exposed Pacific coastline at Hernani (Fig. 2c), some 45 km north of the typhoon track, significant storm-wave contributions resulted in high water marks exceeding 7 m. Further amplification by the wave run-up on steep slopes such as near Guiuan resulted in a maximum run-up height of 14 m (Tajima et al. 2014). Surge heights exceeding 5 m were recorded along the shores of San Pedro Bay. We detail the nature of the storm surge in San Pedro Bay, where the highest death toll was recorded, in the next section. Outside of San Pedro Bay, but still within Leyte Gulf, the surge heights were only 3–4 m between Marabut and Quinapondan (Fig. 2b) because the storm track was parallel to the coastline. Water marks as high as 5 m were attributed to storm-wave contributions. In close proximity to Haiyan's landfall location between Tolosa and Dulag, the surge heights ranged between 3 and 5 m (Fig. 2a). At an exceptional site in Dulag, a 7-m-high water mark was compromised by significant storm-wave contribution. The lowest surge height of about 2 m was recorded at General MacArthur on the eastern coast of Samar (Fig. 2c). The site is sheltered behind fringing coral reefs located 3 km offshore and is on a bay with a narrow bottleneck entrance attenuating storm waves and resulting in a measurement dominated by the storm surge component.

Storm surge simulations of Typhoon Haiyan and Ty 1897 in San Pedro Bay. The Haiyan storm surge modeling results resolved an initial sea level drawdown around 2130 UTC 7 November 2013 (0530 PHT 8 November) in accordance with eyewitness accounts and the Tacloban tide gauge recording (Fig. 4). The tide gauge recorded a drawdown of at least 0.8 m before it broke down,[2] while modeling suggests a drawdown of at least 1.2 m at the head of San Pedro Bay (Figs. 4a,b). The initial sea level drawdown was also observed at Basey on Samar (Amadore 2013). The drawdown was generated by persistent, strong, northerly offshore winds that initially drove the waters southward out of San Pedro Bay (Figs. 4a,b). Similar sea level drawdowns or negative surges from strong offshore winds during historic hurricanes have also been reported for the western Florida coasts (Harris 1963; Lawrence and Cobb 2005). The drawdown exposed

[2] The Tacloban tide data were provided by the National Mapping and Resources Information Agency (NAMRIA) of the Republic of the Philippines.

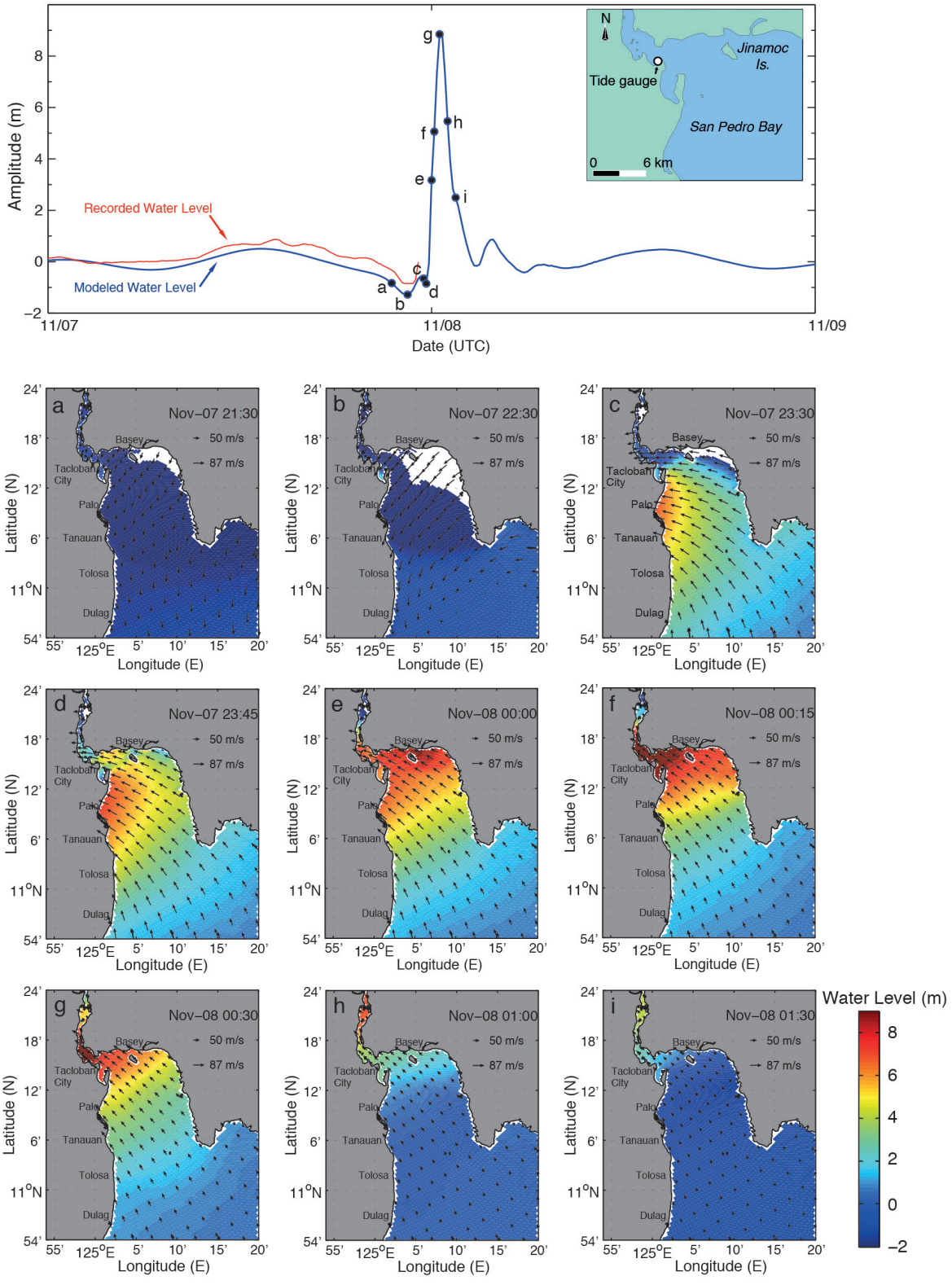

Fig. 4. Sea level heights in Tacloban and nearby coasts around San Pedro Bay during Typhoon Haiyan. (top) Graphical representation of the water levels from storm surge model (blue line) and from Tacloban Port tide gauge (red line). Both the actual and modeled tides show receding sea level prior to the peak surge. (a)–(i) Storm surge model sequence of Typhoon Haiyan in San Pedro Bay from 2130 UTC 7 Nov to 0130 UTC 8 Nov 2013 with colors and arrows representing water level and wind magnitude and direction, respectively.

the seafloor and dramatically steepened the storm tide profile. This phenomenon is analogous to the negative leading N-wave during tsunamis, usually resulting in a higher run-up (Tadepalli and Synolakis 1994). Eyewitness accounts and modeling show that the storm tide arrived as an unusually fast-moving "tsunami like" wave front, which caused high velocity coastal flooding to heights of more than 7 m near Tacloban and Basey. Residents in Basey, who stayed in their homes despite prior evacuation warnings, described a large wave similar to a tsunami striking soon after the water receded, providing only a few minutes of lead time to seek refuge at higher elevations.

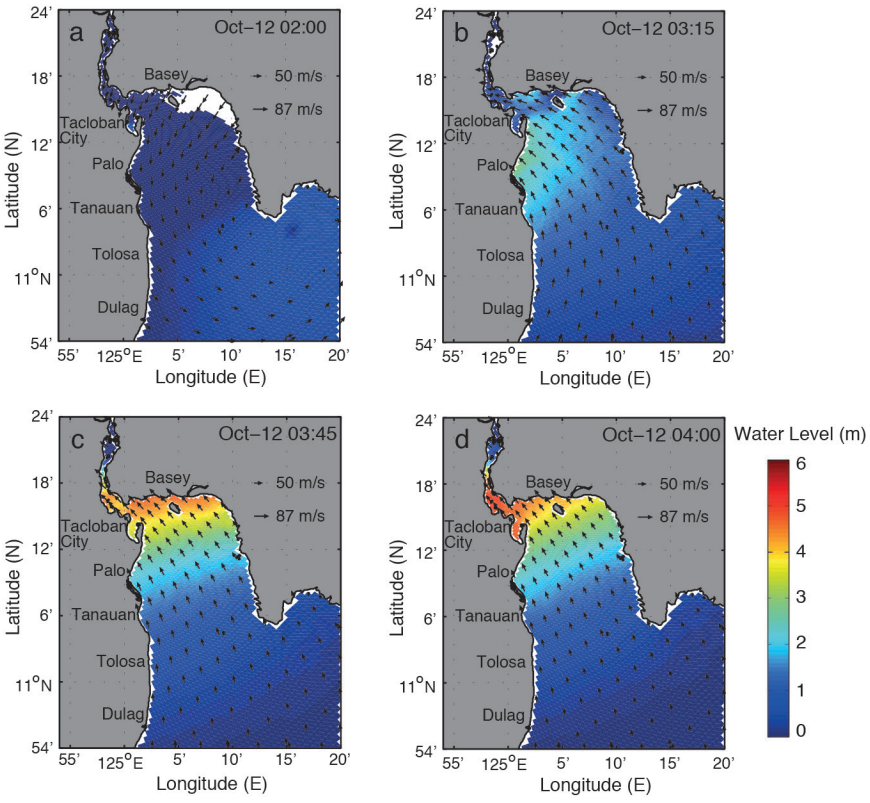

Fig. 5. Storm surge model sequence of Ty 1897 in San Pedro Bay from 0200 to 0400 UTC 12 Oct 1897 with colors and arrows representing water level and wind magnitude and direction, respectively.

The initial rise, peak, and lowering of flood levels due to the storm surge varied considerably in time and location. In downtown Tacloban, the peak surge occurred around 0000 UTC 8 November (0800 PHT 8 November), according to videos recorded by several eyewitnesses and the detailed coverage by storm chaser Morgerman (2014). The inundation timing was further confirmed by two wall clocks located about 14 km apart along the western shores of San Pedro Bay, which were stopped as seawater floods reached about 1.5–2 m high. In Tanauan, the clock stopped at 0720 PHT (2320 UTC 7 November); the clock in Tacloban City stopped a few minutes later at 0730 PHT (2330 UTC 7 November). The timing from the videos and wall clocks is consistent with the storm surge model. The modeled timing of the peak surge coincided with the timing of the onshore-directed winds closely linked to the forward motion of Typhoon Haiyan (Figs. 4c–g). The modeled peak surge of 6–8 m in San Pedro Bay occurred between 0000 and 0030 UTC (0800 and 0830 PHT) 8 November, arrived earlier along the eastern shores at the entrance of the bay, and propagated northward to the bay head. It is likely that several eyewitnesses in Dulag observed the front of the storm surge. During the passage of the eye (calm winds), eyewitnesses saw an offshore "wall of water" about 6 m high that first was moving west toward Dulag but then suddenly redirected north toward Tacloban. The peak surge lasted for at least 30 min, and then just before 0100 UTC (0900 PHT) 8 November, the water subsided (Figs. 4h–i).

In addition, the modeled water level in Fig. 4 shows three apparent peaks corresponding to points C, G, and after point I. The peaks may coincide with the three "waves" reported by eyewitnesses (Amadore 2013; Morgerman 2014), although the timing could not be verified since the eyewitnesses did not track the timing of the three waves. In the open sea coast of Hernani, accounts of the storm surge coming in three waves also exist. The video footage from Hernani showed the building collapsing with the impact of the second wave, which corresponds to the highest and steepest peak in the storm surge model in San Pedro Bay.

The storm surge simulation of Ty 1897 (Fig. 5) showed water levels and peak surge timing that are consistent with Algué's report (see the supplemental information online at http://dx.doi.org/10.1175/BAMS-D-14-00245.2). In Basey, north-northeasterly offshore winds forced the water to

recede (Fig. 5a). The initial rise of the surge occurred with the east-southeasterly winds (Fig. 5b), whereas south-southeasterly winds caused the peak surge in Tacloban and Basey (Figs. 5c,d). On the contrary, in Tolosa the model did not absolutely replicate the actual surge height. Algué reported surge height of ~3 m, but the model yielded 2 m. The discrepancy can be attributed to various factors including changes in nearshore bathymetry, storm-wave contribution, and uncertainties in the Ty 1897 typhoon parameters. For the most part of San Pedro Bay, the modeled surges indicate that Ty 1897 generated lower surge heights than Typhoon Haiyan (Fig. 6), which is consistent with the field measurements for both storm surge events. The magnitude difference of the modeled surge heights between the two typhoons (Fig. 7) is also consistent with the magnitude difference of the measured water levels in both posttyphoon surveys.

IMPLICATIONS FOR DISASTER MANAGEMENT. *Understanding the local storm surge hazard.* The complex interactions among several factors including typhoon intensity represented by the lowest pressure and maximum wind speed, forward movement of the typhoon, storm size, bathymetry, coastline shape, and tidal phase result in varying storm surge height and flooding duration for any storm (e.g., Emanuel 2005a; Irish et al. 2008; Needham and Keim 2014). Given the similar areas impacted by the storm surges of Ty 1897 and Typhoon Haiyan, the coastal geomorphology is assumed to be relatively constant for these two events. Lander et al. (2014) estimated a 20-cm sea level rise between 1970 and 2013, which likely did not contribute significantly to the impact of the storm surge from Typhoon Haiyan. The effect of sea level rise on the tidal phases of Ty 1897 and Typhoon Haiyan is beyond the scope of this study. We focused on differences in typhoon characteristics including track, intensity, size, and forward movement and their possible effect on the storm surge characteristics.

Despite the atmospheric differences between Ty 1897 and Typhoon Haiyan, the resulting two storm surges share notable similarities dictated by the local coastal configuration (Fig. 2). At exposed locations like Hernani, both typhoons generated peak surges exceeding 7 m with significant storm-wave contributions superimposed on top of the surge. In stark contrast, sheltered locations such as General MacArthur experienced the lowest flood levels with 2-m peak surges. Another similarity in both typhoons was the water receding off Basey in San Pedro Bay prior to the peak surge. Based on the historical accounts and our simulations, the 1.2-km-wide strait separating Jinamoc Island from Basey can be exposed as the water recedes prior to the peak surge given the shallow-water depth of ~1.5 m under normal conditions. In both typhoons, the surge in San Pedro Bay initially rose just before the typhoon made landfall on Leyte Island with easterly onshore winds. The surge then peaked with the southeasterly onshore winds as the typhoon eye

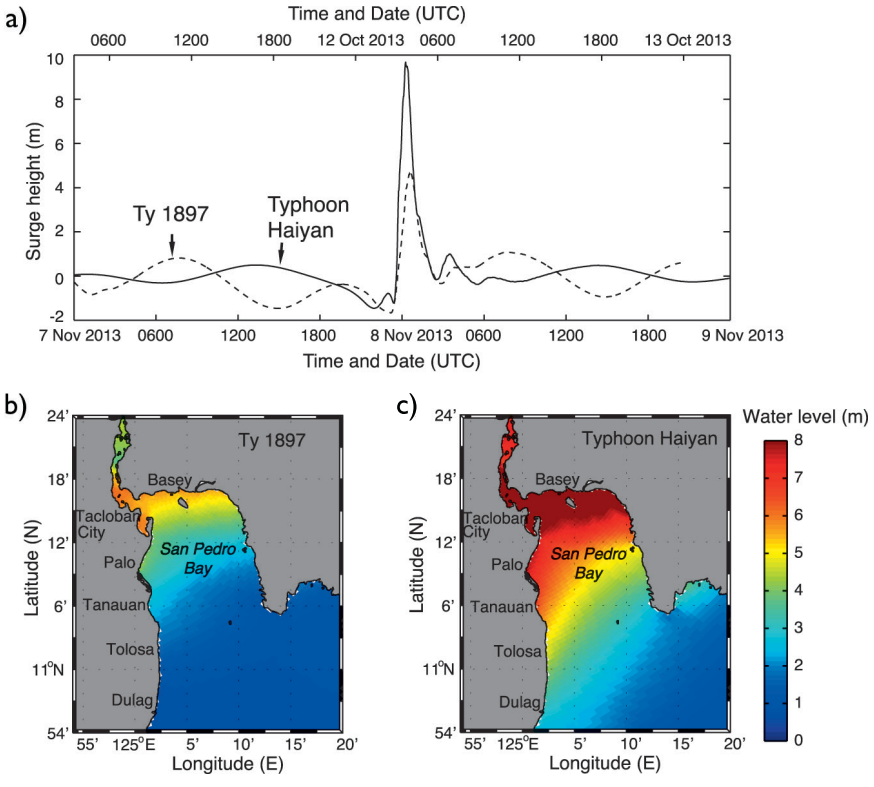

Fig. 6. Modeled surge heights comparison between Ty 1897 and Typhoon Haiyan in San Pedro Bay. (a) Graphical representation of the modeled water level at Tacloban for Ty 1897 and Typhoon Haiyan. (b) Modeled maximum surge heights in San Pedro Bay during Ty 1897. (c) Modeled maximum surge heights in San Pedro Bay during Typhoon Haiyan.

moved west toward the interior of Leyte Island (Figs. 4, 5).

Irrespective of the coastal configuration, whether in exposed open sea (e.g., Hernani) or in a sheltered embayment (e.g., San Pedro Bay), the typhoon forward motion resulted in significantly different peak flooding duration between the two storm surge events. The slower forward motion of Ty 1897 resulted in longer peak floods lasting for about 3 h. In contrast, the much-faster-moving Typhoon Haiyan resulted in rapid high velocity peak floods spanning about 30 min to nearly 1 h.

The higher and more extensive peak surge around San Pedro Bay during Typhoon Haiyan compared to Ty 1897 (Fig. 6) could be due to the latitudinal shift of the typhoon tracks, differences in the intensity and forward motion of these two typhoons, or a combination of these factors. The northerly track of Ty 1897 made Tanauan the landfall location, reducing the surge near Palo and Tanauan; this is true especially given the relative absence of strong onshore winds when compared to Typhoon Haiyan. Meanwhile, the relatively more intense and larger Typhoon Haiyan generated stronger onshore winds on the northern and western shores of San Pedro Bay. The stronger onshore winds in turn induced surge heights almost twice those of Ty 1897, thereby extending over a wider region (Fig. 6).

Apart from typhoon intensity, the storm size was recognized as an additional important factor in generating high storm surges and extensive inundation during Hurricane Katrina (Irish et al. 2008). Given the geometry of San Pedro Bay, however, the storm size might not be an equally significant factor in generating high storm surges in the case of Typhoon Haiyan. The distance from the Typhoon Haiyan track to the head of San Pedro Bay is ~40 km, which is well within the zone of maximum winds. Although when considering the more southerly track of Typhoon Haiyan, the storm size likely contributed to the extreme surge heights along the more exposed coasts of eastern Samar such as at Hernani.

Multihazard evacuation strategies. Figure 8 shows the damage from Typhoon Haiyan surrounding San Pedro Bay. In the northern part of Tacloban, including the downtown area, the landward limit of inundation during Typhoon Haiyan exceeded 500 m (Tajima et al. 2014). Along low-lying, swampy areas south of downtown Tacloban, and similarly at Tanauan, inundation extended more than 2-km inland. Overland flooding reached over 2 km, but the primary areas of damage were concentrated within 200 m of the coast, highlighting that the destructive power of storm

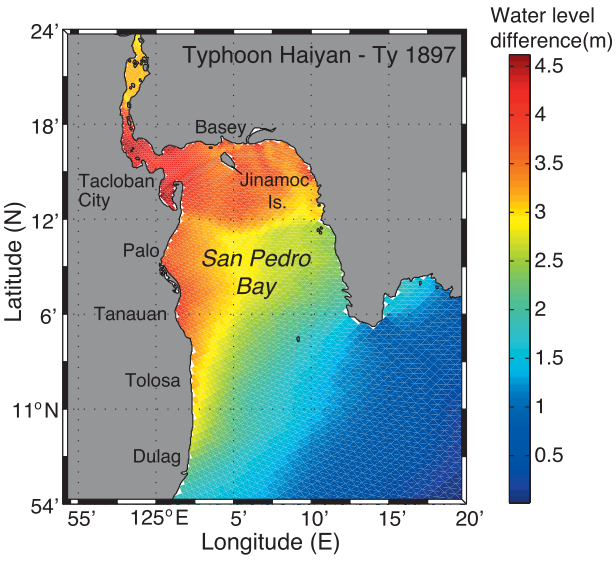

Fig. 7. Difference in water levels of the modeled maximum surge height between Ty 1897 and Typhoon Haiyan in San Pedro Bay.

waves riding on top of the storm surge has a limited inland penetration [Federal Emergency Management Agency (FEMA 2011). Very few structures withstood the energy of the storm surge and superimposed storm waves (Figs. 8b,c,d,f). In areas above the surge heights, extreme typhoon winds caused greater damage, destroying roofs and wide swaths of coconut trees (Fig. 8e). Therefore, the combined hazards from storm surge flooding, extreme winds, and the prevailing vulnerabilities must be considered when developing appropriate evacuation strategies.

Typhoon warning and response. The Philippine government issued typhoon forecasts and warnings for evacuations at least 18 h before Typhoon Haiyan's landfall to achieve minimum and possibly zero casualties from the imminently approaching cyclonic storm threat (Ranada 2013; NDRRMC 2013c; IRIDeS 2014). Preliminary social surveys suggest that local residents had a mixed response to the typhoon warnings emerging from complex social concerns (IRIDeS 2014; Leelawat et al. 2014). These studies highlight that communication pathways, warning systems, evacuation plans, and multilevel hazard and disaster perception were significant concerns for evacuation decisions among individuals in the areas severely impacted by Typhoon Haiyan. These findings underscore the need for the authorities responsible for disseminating weather warnings to better understand how typhoon warnings are transmitted from an initial source through intermediate relays to the final recipients, as well as how the potentially vulnerable

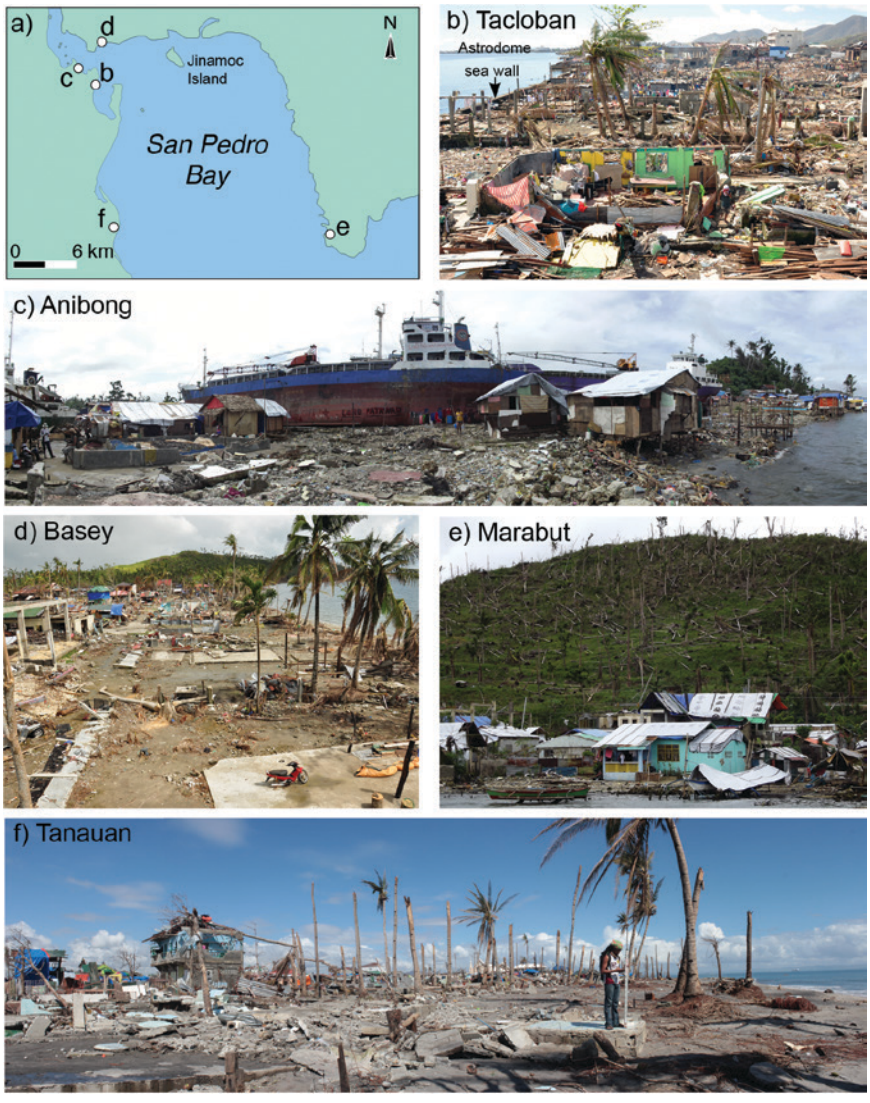

Fig. 8. Photos of storm damage around San Pedro Bay. (a) Location map. Most structures proximal to the coast in (b) Tacloban, (d) Basey, and (f) Tanauan were completely destroyed by the storm surge and the overriding storm waves. Like in most coastal settlements, existing guidelines on foreshore easement[3] were completely ignored. (c) In Anibong village, just north of downtown Tacloban, stilt houses are rebuilt seaward of the stranded ships 2 months after the event. (e) In Marabut, wide swaths of palm trees chopped by the extreme winds.

residents receive, heed, interpret, and decide to act upon these warnings.

Given the historical perspective of storm surge hazards discussed in this paper, social scientists and historians may be able to improve local historical awareness about previous typhoon experiences to aid in hazard perception and response. Historical records show that several tropical cyclones have made landfall in the area surrounding Leyte Gulf (Fig. 9; Tables 3 and 4). According to an unpublished data of PAGASA4, nine of the tropical cyclones have generated storm surges (Table 3). Among these storms, residents identify the November 1984 Typhoon Agnes and the associated coastal flooding of more than 2-m deep in Samar and Leyte as the worst in living memory (e.g., Amadore 2013). Leik et al. (1981) noted that many people along the Gulf and Atlantic coasts in the United States have incorrectly believed that they have been through major cyclonic events, although Baker (1991) recognized that defining and measuring hurricane experience is a difficult task. Of particular relevance to the Philippines, several residents on Leyte and Samar Islands admitted that their experience of past typhoons misled them to believe that an evacuation lead time of minutes would be sufficient. This raises a long-lasting question: How does the experience of smaller, relatively less impactful events shape the response of the community to larger, unprecedented events or those with return periods outside the living memory of residents?

On a broader note, although stronger prehistoric events (Donnelly et al. 2006; Nott 2007) remain to be explored, and as long as other historical events remain unverified, the Ty 1897 and Typhoon Haiyan storm surges may serve as worst-case scenarios for this region. These rare but disastrous events should be carefully evaluated toward enhancing community-based disaster risk awareness, planning, and response.

[3] The Water Code of the Philippines (Presidential Decree 1067) designates an easement of 40 m from seashore. This is supposed to be a "no build zone" area.

CONCLUSIONS.

Historical records reveal a predecessor to Typhoon Haiyan occurred on 12 October 1897. This typhoon, referred to here as Ty 1897, took a similar path of destruction through the eastern central Philippines. Ty 1897 and Haiyan had almost identical typhoon tracks, but Typhoon Haiyan was more intense, had larger maximum wind coverage, and moved faster than Ty 1897. Our combined field observations, eyewitness accounts, and computer simulations consistently indicate that Typhoon Haiyan's storm surge was about twice the height of the 1897 event in San Pedro Bay, but the two storm surges had similar heights on the open Pacific coast such as at Hernani. While stronger prehistoric events remain unexplored, Ty 1897 and Typhoon Haiyan storm surges may serve as extreme scenarios for this region in terms of disaster risk awareness, planning, and response.

TABLE 3. Tropical cyclones with known storm surge occurrence (represented as white solid lines in Fig. 9).

No.	Name	Date	Max winds (kt)[a]	Min pressure (hPa)
1	No name	12 Oct 1897		(694 mm[b,c]) 925
2	No name	4 May 1913		(727.8 mm[c]) 970
3	No name	3 Jun 1923		(739.52 mm[c]) 973
4	26W	14 Dec 1948	35[a, JTWC]	
5	Wanda	23 Apr 1971	40[a, JMA]	993[a, JMA]
6	Agnes	4 Nov 1984	100[a, JMA]	925[a, JMA]
7	Skip	7 Nov 1988	70[a, JMA]	955[a, JMA]
8	Mike	12 Nov 1990	90[a, JMA]	935[a, JMA]
9	Haiyan	8 Nov 2013	125[a, JMA]	895[a, JMA]

TABLE 4. Tropical cyclones with unknown storm surge occurrence (represented as white dashed lines in Fig. 9).

No.	Name	Date	Max winds (kt)[a]	Min pressure (hPa)
1	No name	24 Nov 1912[d]		(693.08 mm[e]) 923
2	Wanda	20 Nov 1951	90[a, JTWC]	985[a, JMA]
3	Wilma	27 Oct 1952	130[a, JTWC]	930[a, JMA]
4	Tilda	29 Nov 1954	120[a, JTWC]	980[a, JMA]
5	Irma	15 May 1966	100[a, JTWC]	974[a, JMA]
6	Jean	14 July 1971	75[a, JTWC]	980[a, JMA]
7	Kit	7 Jan 1972	75[a, JTWC]	975[a, JMA]
8	Nelson	25 Mar 1982	105[a, JTWC]	940[a, JMA]
9	Axel	21 Dec 1994	95[a, JTWC]	960[a, JMA]

[a] IBTrACS database of Knapp et al. (2010) using either JTWC or JMA data.

[b] Data of Algué (1898).

[c] Data of Algué (1904).

[d] This Nov 1912 typhoon is believed to be deadly (http://chroniclingamerica.loc.gov/lccn/sn83045433/1912-11-30/ed-1/seq-1/), but other reports on the damage and impact to human life were insufficient for verification (U.S. War Office 1913).

[e] Data of Selga (1935).

ACKNOWLEDGMENTS. This research is supported by the National Research Foundation Singapore under its Singapore NRF Fellowship scheme (National Research Fellow Award NRF-RF2010-04) and administered by Earth Observatory of Singapore and the National Research Foundation Singapore and the Singapore Ministry of Education under the Research Centres of Excellence initiative. Additional funding for the Filipino scientists has come from the Department of Science and Technology, the Philippines. We thank Antonia

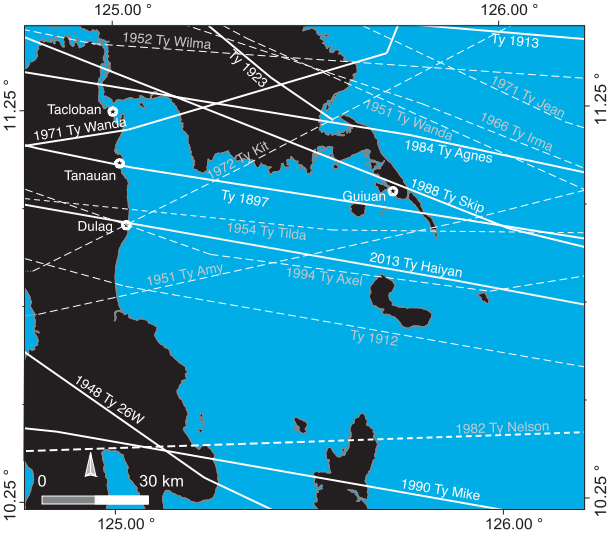

FIG. 9. Landfalling tropical cyclones in the surrounding area of Leyte Gulf between 1897 and 2013. Storm tracks were from the IBTrACS database of Knapp et al. (2010). The attributes of each typhoon are summarized in Tables 3 and 4.

Yulo-Loyzaga of Manila Observatory, who provided the Algué report. We acknowledge John Elton Chua, Livre Lacierda, Mark Anthony Bamba, Mikko Garcia, Angel Doctor, and Sorvigenaleon Ildefonso for helping us gather data in the field. We are grateful to Chris Landsea and three anonymous reviewers, whose comprehensive and insightful reviews significantly improved the manuscript. Comments from Kelvin Rodolfo, Chris Gouramanis, and Aron Meltzner were valuable in refining the final version.

REFERENCES

Algué, J., 1898: El baguio de Samar y Leyte, 12–13 de Octubre de 1897. Manila Observatory, 74 pp.

——, 1904: *The Cyclones of the Far East.* Bureau of Public Printing, 283 pp.

Alojado, D., and D. M. Padua, 2010: Worst typhoons of the Philippines 1947–2009. Accessed 06 July 2014. [Available online at www.typhoon2000.ph/stormstats/WorstPhilippineTyphoons.htm.]

Amadore, L. A., 2013: Storm surge in Basey, Samar. Accessed 03 April 2013. [Available online at http://opinion.inquirer.net/66477/storm-surge-in-basey-samar.]

Atkinson, G. D., and C. R. Holliday, 1977: Tropical cyclone minimum sea level pressure/maximum sustained wind relationship for the western North Pacific. *Mon. Wea. Rev.*, **105**, 421–427, doi:10.1175/1520-0493(1977)105<0421:TCMSLP>2.0.CO;2.

Bacani, L., 2013: Deadliest, most destructive cyclones of the Philippines. Accessed 11 July 2014. [Available online at www.philstar.com/headlines/2013/11/11/1255490/deadliest-most-destructive-cyclones-philippines.]

Baker, E. J., 1991: Hurricane evacuation behavior. *Int. J. Mass Emerg. Disasters*, **9**, 287–310.

Bricker, J., H. Takagi, E. Mas, S. Kure, B. Adriano, C. Yi, and V. Roeber, 2014: Spatial variation of damage due to storm surge and waves during Typhoon Haiyan in the Philippines. *J. Japan Soc. Civil Eng.*, **70**, 2, I_231–I_235.

Caulderwood, K., 2014: The ten most expensive natural disasters in 2013. Accessed 03 March 2014. [Available online at www.ibtimes.com/report-ten-most-expensive-natural-disasters-2013-1540058.]

Donnelly, C., N. Kraus, and M. Larson, 2006: State of knowledge on measurement and modeling of coastal overwash. *J. Coastal Res.*, **22**, 965–991, doi:10.2112/04-0431.1.

Dvorak, V. F., 1975: Tropical cyclone intensity analysis and forecasting from satellite imagery. *Mon. Wea. Rev.*, **103**, 420–430, doi:10.1175/1520-0493(1975)103<0420:TCIAAF>2.0.CO;2.

——, 1984: Tropical cyclone intensity analysis using satellite data. NOAA Tech. Rep. NESDIS 11, 50 pp. [Available online at ftp://satepsanone.nesdis.noaa.gov/Publications/Tropical/Dvorak_1984.pdf.]

Egbert, G. D., and S. Y. Erofeeva, 2002: Efficient inverse modeling of barotropic ocean tides. *J. Atmos. Oceanic Technol.*, **19**, 183–204, doi:10.1175/1520-0426(2002)019<0183:EIMOBO>2.0.CO;2.

Emanuel, K. A., 2005a: The storm surge. *Divine Wind: The History and Science of Hurricanes*. Oxford University Press, 147–152.

——, 2005b: The hunters. *Divine Wind: The History and Science of Hurricanes*. Oxford University Press, 193–202.

FEMA, 2011: Coastal construction manual: Principles and practices of planning, siting, designing, constructing, and maintaining residential buildings in coastal areas. U.S. Department of Homeland Security FEMA P-55, Vol. 1, 242 pp.

Flater, D., 1998: XTide: Harmonic tide clock and tide predictor. Accessed 25 May 2014. [Available online at www.flaterco.com/xtide/.]

Fritz, H. M., and Coauthors, 2007: Hurricane Katrina storm surge distribution and field observations on the Mississippi Barrier Islands. *Estuarine Coastal Shelf Sci.*, **74**, 12–20, doi:10.1016/j.ecss.2007.03.015.

——, C. D. Blount, S. Thwin, M. K. Thu, and N. Chan, 2009: Cyclone Nargis storm surge in Myanmar. *Nat. Geosci.*, **2**, 448–449, doi:10.1038/ngeo558.

——, and Coauthors, 2012: The 2011 Japan tsunami current velocity measurements from survivor videos at Kesennuma Bay using LiDAR. *Geophys. Res. Lett.*, **39**, L00G23, doi:10.1029/2011GL050686.

Harris, D. L., 1963: Characteristics of the hurricane storm surge. U.S. Department of Commerce Weather Bureau Tech. Paper 48, 19–24. [Available online at https://coast.noaa.gov/hes/images/pdf/CHARACTERISTICS_STORM_SURGE.pdf.]

Holland, G. J., 1980: An analytic model of the wind and pressure profiles in hurricanes. *Mon. Wea. Rev.*, **108**, 1212–1218, doi:10.1175/1520-0493(1980)108<1212:AAMOTW>2.0.CO;2.

IRIDeS, 2014: Initial Report of International Research Institute of Disaster Science (IRIDeS): IRIDeS Fact-Finding Missions to Philippines. Tohoku University, 105 pp.

Irish, J. L., D. T. Resio, and J. J. Ratcliff, 2008: The influence of storm size on hurricane surge. *J. Phys. Oceanogr.*, **38**, 2003–2013, doi:10.1175/2008JPO3727.1.

Joint Typhoon Warning Center, 2014: JTWC western North Pacific best track data 2013. Joint Typhoon Warning Center, accessed 10 July 2014. [Available

online at www.usno.navy.mil/NOOC/nmfc-ph/RSS/jtwc/best_tracks/wpindex.php.]

Knaff, J. A., and R. M. Zehr, 2007: Reexamination of tropical cyclone wind-pressure relationships. *Wea. Forecasting*, **22**, 71–88, doi:10.1175/WAF965.1.

Knapp, K. R., and M. C. Kruk, 2010: Quantifying interagency differences in tropical cyclone best track wind speed estimates. *Mon. Wea. Rev.*, **138**, 1459–1473.

Knapp, K. R., M. C. Kruk, D. H. Levinson, H. J. Diamond, and C. J. Neumann, 2010: The International Best Track Archive for Climate Stewardship (IBTrACS): Unifying tropical cyclone best track data. *Bull. Amer. Meteor. Soc.*, **91**, 363–376, doi:10.1175/2009BAMS2755.1.

Koba, H., T. Hagiwara, S. Asano, and S. Akashi, 1990: Relationships between CI number from Dvorak's technique and minimum sea level pressure or maximum wind speed of tropical cyclone (in Japanese). *J. Meteor. Res.*, **42**, 59–67.

Kruk, M. C., K. R. Knapp, and P. A. Hennon, 2011: On the use of the Dvorak current intensity as a climate data record in the western North Pacific. *23rd Conf. on Climate Variability and Change*, Seattle, WA, Amer. Meteor. Soc., 142. [Available online at https://ams.confex.com/ams/91Annual/webprogram/Paper179185.html.]

Lander, M., C. Guard, and S. J. Camargo, 2014: Super Typhoon Haiyan [in "State of the Climate 2013"]. *Bull. Amer. Meteor. Soc.*, **95** (7), S112–S114.

Lawrence, H., and H. Cobb, 2005: Tropical cyclone report: Hurricane Jeanne, 13-28 September 2004. Accessed 11 March 2014. [Available online at www.nhc.noaa.gov/data/tcr/AL112004_Jeanne.pdf.]

Leelawat, N., C. M. R. Mateo, S. M. Gaspay, A. Suppasri, and F. Imamura, 2014: Filipinos' views on the disaster information for the 2013 Super Typhoon Haiyan in the Philippines. *Int. J. Sustainable Future Hum. Secur.*, **2** (2), 16–28.

Leik, R. K., T. M. Carter, J. P. Clark, S. D. Kendall, and G. A. Gifford, 1981: Community response to natural hazard warnings. Summary Final Rep. DCPA01-79-C-0214, FEMA Work Unit 2234-F, 77 pp. [Available online at http://oai.dtic.mil/oai/oai?verb=getRecord&metadataPrefix=html&identifier=ADA099509.]

Lesser, G. R., J. A. Roelvink, J. A. T. M. van Kester, and G. S. Stelling, 2004: Development and validation of a three-dimensional morphological model. *Coastal Eng.*, **51**, 883–915, doi:10.1016/j.coastaleng.2004.07.014.

Mas, E., J. Bricker, S. Kure, B. Adriano, C. Yi, A. Suppasri, and S. Koshimura, 2015: Field survey report and satellite image interpretation of the 2013 Super Typhoon Haiyan in the Philippines. *Nat. Hazards Earth Syst. Sci.*, **15**, 805–816, doi:10.5194/nhess-15-805-2015.

Morgerman, J., 2014: Super Typhoon HAIYAN in Tacloban City & Leyte, Philippines: Data & documentation from the landfall zone of a category-5 cyclone. iCyclone Rep., 47 pp. [Available online at www.icyclone.com/upload/now/apr_2014/iCyclone_HAIYAN_in_Tacloban_City_040314.pdf.]

Mori, N., M. Kato, S. Kim, H. Mase, Y. Shibutani, T. Takemi, K. Tsuboki, and T. Yasuda, 2014: Local amplification of storm surge by Super Typhoon Haiyan in Leyte Gulf. *Geophys. Res. Lett.*, **41**, 5106–5113, doi:10.1002/2014GL060689.

Nakazawa, T., and S. Hoshino, 2009: Intercomparison of Dvorak parameters in the tropical cyclone datasets over the western North Pacific. *SOLA*, **5**, 33–36, doi:10.2151/sola.2009-009.

National Mapping and Resource Information Authority, 1980: Nautical chart of San Pedro Bay. 1:402000. Sheet 4468.

NDRRMC, 2013a: Preparations for Typhoon "YOLANDA" (HAIYAN). NDRMMC Situational Rep. 2, 10 pp. [Available online at www.ndrrmc.gov.ph/attachments/article/1329/Preparations_for_Typhoon_YOLANDA_(HAIYAN)_SitRep_No_02_07NOV2013_0600H.pdf.]

——, 2013b: Effects of Typhoon "YOLANDA" (HAIYAN). NDRRMC Situational Rep. 10, 43 pp. [Available online at www.ndrrmc.gov.ph/attachments/article/1329/Effects_of_Typhoon_YOLANDA_(HAIYAN)_SitRep_No_10_10NOV2013_0600H.pdf.]

——, 2013c: Preparations for Typhoon "YOLANDA" (HAIYAN). NDRMMC Situational Rep. 3, 13 pp. [Available online at www.ndrrmc.gov.ph/attachments/article/1329/Preparations_for_Typhoon_YOLANDA_(HAIYAN)_SitRep_No_03_07NOV2013_0000H.pdf.]

——, 2014: Effects of Typhoon "YOLANDA" (HAIYAN). Situational Rep. 108, 67 pp. [Available online at www.ndrrmc.gov.ph/attachments/article/1329/Effects_of_Typhoon_YOLANDA_(HAIYAN)_SitRep_No_108_03APR2014.pdf.]

Needham, H. F., and B. D. Keim, 2014: Correlating storm surge heights with tropical cyclone winds at and before landfall. *Earth Interact.*, **18**, doi:10.1175/2013EI000527.1.

Nott, J., 2007: The importance of quaternary records in reducing risk from tropical cyclones. *Palaeogeogr. Palaeoclimatol. Palaeoecol.*, **251**, 137–149, doi:10.1016/j.palaeo.2007.02.024.

Paciente, R. B., 2014: Response and lessons learned from Typhoon "Haiyan" (Yolanda). *JMA/WMO Workshop*

on Effective Tropical Cyclone Warning in Southeast Asia, Session 6: Effective Early Warning: Lessons learnt from past TC Disasters. Tokyo, Japan, Japan Meteorological Agency. [Available online at www.jma.go.jp/jma/jma-eng/jma-center/rsmc-hp-pub-eg/2014_Effective_TC_Warning/documents.html.

Ranada, P., 2013: Leyte warned of storm surges. Accessed 10 November 2013. [Available online at www.rappler.com/nation/43179-yolanda-storm-surges.]

Ribera, P., R. García-Herrera, and L. Gimeno, 2008: Historical deadly typhoons in the Philippines. *Weather*, **63**, 194–199, doi:10.1002/wea.275.

Selga, M., 1935: Charts of remarkable typhoons in the Philippines 1902–1934. *Catalogue of Typhoons 1348–1934*, Manila Weather Bureau, 1–55.

Tadepalli, S., and C. E. Synolakis, 1994: The run-up of N-waves on sloping beaches. *Proc. Roy. Soc. London*, **A445**, 99–112, doi:10.1098/rspa.1994.0050.

Tajima, Y., and Coauthors, 2014: Initial report of JSCE-PICE joint survey on the storm surge disaster caused by Typhoon Haiyan. *Coastal Eng. J.*, **56**, 1450006, doi:10.1142/S0578563414500065.

Udías, A., 1996: Jesuits' contribution to meteorology. *Bull. Amer. Meteor. Soc.*, **77**, 2307–2315, doi:10.1175/1520-0477(1996)077<2307:JCTM>2.0.CO;2.

UNESCO, 2014: International Tsunami Survey Team (ITST) post-tsunami survey guide. UNESCO-IOC Manuals and Guides 37, 114 pp. [Available online at http://unesdoc.unesco.org/images/0022/002294/229456E.pdf.]

U.S. War Office, 1913: Typhoons. *Report of the Philippine Commission to the Secretary of War*, Washington Government Printing Office, 32.

Velden, C., and Coauthors, 2006: The Dvorak tropical cyclone intensity estimation technique: A satellite-based method that has endured for over 30 years. *Bull. Amer. Meteor. Soc.*, **87**, 1195–1210, doi:10.1175/BAMS-87-9-1195.

World Meteorological Organization, 2015: Typhoon committee operational manual: Meteorological component. Tropical Cyclone Programme Rep. TCP-23, 169 pp. [Available online at www.wmo.int/pages/prog/www/tcp/documents/TCP-23EDITION2015.pdf.]